Adaptive Predictive-DPC for LCL-Filtered Grid Connected VSC with Reduced Number of Sensors

Gholami-Khesht, Hosein; Davari, Pooya; Blaabjerg, Frede

Published in:
The 22nd European Conference on Power Electronics and Applications (EPE'20 ECCE Europe)

DOI (link to publication from Publisher):
10.23919/EPE20ECCEEurope43536.2020.9215839

Publication date:
2020

Document Version
Early version, also known as pre-print

Adaptive Predictive-DPC for LCL-Filtered Grid Connected VSC with Reduced Number of Sensors

Hosein Gholami-Khesht, Pooya Davari, Frede Blaabjerg
Department of Energy Technology, Aalborg University, Aalborg, Denmark
hgk@et.aau.dk, pda@et.aau.dk, fbl@et.aau.dk

Acknowledgements

The work is supported by the Reliable Power Electronic-Based Power System (REPEPS) project at the Department of Energy Technology, Aalborg University as a part of the Villum Investigator Program funded by the Villum Foundation.

Keywords

«Voltage source converter (VSC)», «Direct power control», «Model-based predictive control (MPC) », «Adaptive control».

Abstract

An adaptive predictive direct power control (P-DPC) method using a Luenberger observer is proposed in conjunction with conventional P-DPC, which reduces the system sensitivity to parameter mismatches and control delays. Moreover, the observer facilitates sensorless operation of the proposed method. The performance of the proposed adaptive P-DPC is confirmed under various simulation and experimental tests.

Introduction

The control of renewable energy-based power generation systems has attracted considerable attention in recent years. Major control goals are the bidirectional and decoupled active and reactive power control as well as sinusoidal current generation [1]-[15]. Basically, power control methods can be divided into two main categories: indirect and direct power control methods [1]-[14]. The proportional-integral (PI) [4]-[5] and the proportional-resonant (PR) [6]-[7] current controllers are the most popular indirect power control methods. The necessity of using a phase-locked loop (PLL), sensitivity to power grid conditions, and inappropriateness for digital implementation are the main disadvantages of these methods. Switching table based direct power control (ST-DPC) [8]-[10] and predictive based direct power control (P-DPC) [11]-[14] are two traditionally used direct power control methods.
Recently methods based on the predictive control theory have become more popular owing to the various advantages they offer [1]-[3], [11]-[14]. A simple structure, simplicity in digital implementation, coincident to the discrete nature of power electronic converters, and superior dynamic and steady-state performance are the most interesting features of the predictive based control methods. In spite of these advantages, sensitivity to control system delays and parameter mismatches may degrade their performance and even cause instability. These problems can be amplified in systems with higher-order filters, while such systems have many advantages, and they are increasingly used day by day [2]-[4], [9]-[10]. Moreover, in predictive control methods, it is necessary to measure all system states to minimize the steady-state errors, and to do better disturbance rejection [2]-[3]. However, measuring all signals with related sensors increases system cost, volume, and weight. As discussed in [2]-[3], the MPC based direct and indirect power control of an LCL-filtered grid-connected voltage source converter (VSC) needs four current and voltage sensors, which may worsen the system reliability due to additional physical components, which might be subject to damages and thereby failures.

To overcome these problems, an adaptive predictive-DPC (P-DPC) is proposed in this paper, which combines the P-DPC with an identification technique. So far, various identification techniques are applied in VSC based power applications, where the most important are the Luenberger observer [16]-[17], the sliding mode observer [18], the Kalman filter [19], the neural network [20], the steepest descent [21], and recursive least square estimator [22]. The proposed method utilizes a Luenberger Observer (LO) in the P-DPC structure. The LO is a closed-loop estimator that uses the state-space model of the system to predict the states of the system from the measured inputs and outputs based on the minimization of the difference between the measured and the estimated outputs. Besides high accuracy and reliability, and noise immunity of determined signals by LO, it helps to compensate the control delays, and reduces the sensitivity to system uncertainties by estimating states and disturbance inputs one sampling period ahead. Moreover, contrary to the conventional predictive control methods [2]-[3], which need many sensors, the LO reduces the number of sensors in the proposed control structure by replacing the grid current sensors. It is also worth noting that the proposed P-DPC does not need a PLL, which prevents interaction between different control loops and PLL, and consequently improves the system stability.

In summary, proposing an augmented state-space model of grid-connected VSC with an LCL output filter, incorporating the LO in the P-DPC structure, and investigating the feasibility of practical implementation of the proposed adaptive P-DPC are the most significant contributions of this work.

In the following sections, firstly, the dynamics of a grid-connected three-phase VSC with LCL output filter are described in section II. Section III presents the proposed P-DPC, which includes four main subsections, proposed adaptive-predictive direct power control, LO design, complex power reference calculation, and active damping. After that, to evaluate the performance of the proposed sensorless P-DPC and the conventional one, simulation and experimental results are presented in section IV. Finally, conclusions are drawn in Section V.

System Modeling

Basic model of the grid-connected three-phase VSC

The single line diagram of the grid-connected three-phase VSC, which is studied in this paper is shown in Fig. 1. The system of Fig. 1 includes the power source, the LCL-type filter, and the three-phase VSC. Using the space vector theory, the converter model can be readily presented as:

$$\begin{cases} L_f \dfrac{di_f}{dt} = v_c - v_{inv} \\ C_f \dfrac{dv_c}{dt} = i_g - i_f \end{cases} \tag{1}$$

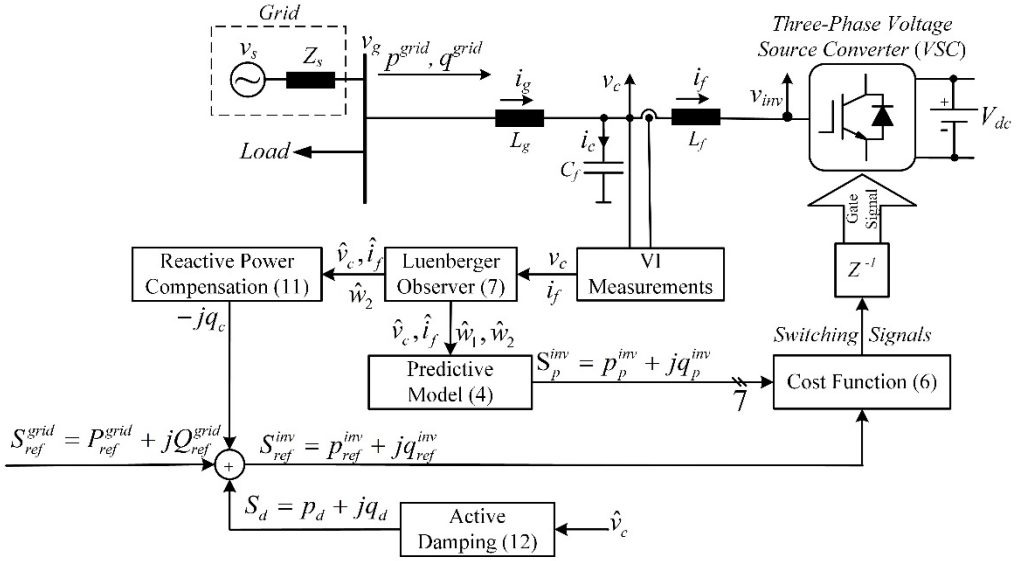

Fig. 1: Proposed adaptive predictive-DPC

where, v_{inv}, v_c, i_f, i_g and i_c are the converter output voltage, capacitor voltage, inverter current, grid current, and capacitor current, respectively. Also, C_f, L_f, and L_g are filter capacitance, inverter-side and grid-side filter inductances.

Augmented state-space model

Generally, the perfect implementation of a model-based predictive control method highly depends on the accuracy of the system model and the parameters' values. However, in practice, the accuracy is subjected to un-modeled dynamics, parameter uncertainties, and external disturbances. In this section, to tackle the problem, an augmented discrete state-space model is used, which includes all system parameters uncertainties and unmodeled dynamics, as follows:

$$\frac{dx(t)}{dt} = Ax(t) + Bu(t) + Dw(t)$$

$$x = \begin{bmatrix} i_f \\ v_c \end{bmatrix}, u = \begin{bmatrix} v_{inv} \end{bmatrix}, w = \begin{bmatrix} w_1 \\ w_2 \end{bmatrix} = \begin{bmatrix} \Delta L_f \dfrac{di_f}{dt} + n_1 \\ i_g + \Delta C_f \dfrac{dv_o}{dt} + n_2 \end{bmatrix}, \tag{2}$$

$$A = \begin{bmatrix} 0 & \dfrac{1}{L_f} \\ \dfrac{-1}{C_f} & 0 \end{bmatrix}, B = \begin{bmatrix} \dfrac{-1}{L_f} \\ 0 \end{bmatrix}, D = \begin{bmatrix} \dfrac{1}{L_f} & 0 \\ 0 & \dfrac{1}{C_f} \end{bmatrix}.$$

where, parameters with and without "Δ" denote the deviation from nominal values and the nominal values, respectively. Also, n_1 and n_2 represent unstructured uncertainties due to un-modeled dynamics and modeling errors. As seen in (2), in the augmented model, all uncertainties caused by parameter mismatches, grid current disturbances, and other unstructured uncertainties are lumped as a disturbance input $w(k)$.

The practical implementation of the predictive control algorithm is based on the discrete state-space model of the plant dynamics. Discretizing (2) with the sampling period T_S, yields the following discrete state-space equations:

$$\begin{cases} x(k+1) = A_d x(k) + B_d u(k) + D_d w(k) \\ A_d = e^{AT_S} = L^{-1}[(\mathrm{s}I - A)^{-1}] \approx I + AT_S \\ B_d = \int_0^{T_S} e^{A_d(T_S-\tau)} B d\tau \approx BT_S \\ D_d = \int_0^{T_S} e^{A_d(T_S-\tau)} D d\tau \approx DT_S \end{cases} \tag{3}$$

Proposed Predictive Direct Power Control (P-DPC)

Proposed adaptive-predictive direct power control

As shown in Fig. 1, the proposed power control contains four main parts: the LO, the model predictive control (MPC), reactive power compensation, and also active damping [4]. The LO provides the predicted states and input disturbances and facilitates a perfect implementation of the MPC by delay compensation of the control system. Based on the augmented model and the predicted variables, the MPC calculates the apparent power for all possible converter voltage vectors and then compares them with the power references. Consequently, the converter voltage vector $(u(k+1))$ that minimizes the error between the predicted and the reference powers is selected and applied at the start of the next sampling period.

To compensate for the inherent delay of digital implementation, the proposed adaptive P-DPC is based on the two-step ahead predicted powers that can be interpreted as:

$$S_p^{inv}(k+2) = p_p^{inv}(k+2) + jq_p^{inv}(k+2) = \hat{v}_c(k+2)\hat{i}_f(k+2)^* \tag{4}$$

where, $S_p^{inv}(k+2)$, $\hat{v}_c(k+2)$ and $\hat{i}_f(k+2)$ are complex power at the beginning of the (k+2)th period, predicted capacitor voltage and inverter current vectors, respectively. Predicted voltage and current vectors are computed from (3) as follows:

$$\hat{x}(k+2) = \begin{bmatrix} \hat{v}_c(k+2) & \hat{i}_f(k+2) \end{bmatrix}^T = A_d\hat{x}(k+1) + B_d u(k+1) + D_d\hat{w}(k+1) \tag{5}$$

In the above equations, $\hat{x}(k+1)$ and $\hat{w}(k+1)$ are estimated signals via the LO that is described in the following subsection.

Finally, by substituting (4) into the cost function of (6), it is evaluated for all possible converter voltage vectors, and then the optimal voltage vector that minimizes the cost function is saved and applied at the beginning of the next sampling period.

$$\begin{cases} g = \left|S_{ref}^{inv}(k+1) - S_p^{inv}(k+2)\right|^2 + \lambda_{sw} g_{sw}{}^2 \\ g_{sw} = \left|SW_a(k+1) - SW_a(k)\right| + \left|SW_b(k+1) - SW_b(k)\right| + \left|SW_c(k+1) - SW_c(k)\right| \end{cases} \tag{6}$$

In (6), $S_{ref}^{inv}(k+1)$ is the reference complex power at the inverter side. Moreover, g_{sw} includes switching efforts to control switching frequency and losses. Also, SW_i (i = a, b, and c) and λ_{sw} are gating signals and weighting factor, respectively [15].

Luenberger observer design

As mentioned in the previous subsection, to evaluate the cost function and accordingly to achieve the optimal converter voltage, the disturbance input and the one sample ahead predicted states are needed. To obtain these quantities, the use of a full-order Luenberger observer is proposed in this subsection. Neglecting the disturbance changes in each sampling period ($w(k+1) \approx w(k)$), the system discrete state-space equation can be rewritten as:

$$\begin{cases} x(k+1) = A_{ob}x(k) + B_{ob}u(k) \\ x(k) = C_{ob}x(k) \end{cases}$$

$$x = \begin{bmatrix} i_f \\ v_c \\ w_1 \\ w_2 \end{bmatrix}, u = \begin{bmatrix} v_{inv} \end{bmatrix}, C_{ob} = \begin{bmatrix} 1 & 0 & 0 & 0 \\ 0 & 1 & 0 & 0 \end{bmatrix}, A_{ob} = \begin{bmatrix} 1 & \frac{T_S}{L_1} & \frac{T_S}{L_1} & 0 \\ \frac{-T_S}{C} & 1 & 0 & \frac{T_S}{C} \\ 0 & 0 & 1 & 0 \\ 0 & 0 & 0 & 1 \end{bmatrix}, B_{ob} = \begin{bmatrix} \frac{-T_S}{L_1} \\ 0 \\ 0 \\ 0 \end{bmatrix} \tag{7}$$

Based on the above equation, a full-order Luenberger observer can be constructed as follows:

$$\hat{x}(k+1) = A_{ob}\hat{x}(k) + B_{ob}u(k) + GC_{ob}(x(k) - \hat{x}(k)) \tag{8}$$

where, symbol "^" denotes the estimated values, and G is the observer gain. The observer gain is chosen such that the estimation error dynamics of (9) is asymptotically stable, and eigenvalues of the observer are placed in the desired locations, as well [16]-[17].

$$\begin{cases} e(k+1) = (A_{ob} - GC_{ob})e(k) \\ e(k) = x(k) - \hat{x}(k) \end{cases} \tag{9}$$

It is worth to notice that the gain matrix of the observer can be calculated to satisfy the mentioned requirements because the observability matrix of the system ($\begin{bmatrix} C_{ob} & C_{ob}A_{ob} \end{bmatrix}^T$) has full column rank.

Complex power reference calculation

In the proposed power controller, the complex power of the inverter side of the LCL-type filter is controlled, while the grid side complex power tracking is desired in most applications. So, if the grid

side power control is required, the inverter side power reference must be simply modified to compensate for the capacitor reactive power, as follows:

$$S_{ref}^{inv}(k+1) = S_{ref}^{grid}(k+1) - jq_c \tag{10}$$

where, $S_{ref}^{inv}(k+1)$, $S_{ref}^{grid}(k+1)$ and q_c are the complex power references of the inverter side and the grid side and the reactive power generated by the capacitor of the LCL-filter, respectively. Based on (1) and (3), the reactive power of the capacitor is calculated as (11).

$$\begin{cases} q_c = v_c(k+1) i_c(k+1)^* \\ i_c(k+1) = w_2(k+1) - i_f(k+1) \end{cases} \tag{11}$$

Active damping

To damp the current oscillation caused by the LCL filter resonance, an active or passive damping method must be used. Work in [9] proposed an effective active damping method that is also employed in this work. Based on this method, the resonance component of the capacitor voltage is extracted to calculate damping components. After that, these derived damping components are added to the power control loop to damp LCL filter resonance.
The damping component can be calculated as:

$$S_d(k+1) = p_d(k+1) + jq_d(k+1) = v_{c,1}(k+1) i_d^*(k+1), \left(i_d = k_d \tilde{v}_c\right) \tag{12}$$

where, $v_{c,1}$ is the fundamental component of the capacitor voltage and $\tilde{v}_c$ is the resonance component of the capacitor voltage. Also, k_d is damping factor. The large value of k_d provides better LCL filter resonance damping, however, it can cause low order harmonic component in the output current, and also output power deviation from the reference one.

Simulation and Experimental Results and Discussion

To evaluate the performance of the proposed adaptive P-DPC under different conditions, a Simulink test bench and laboratory prototype have been prepared, as shown in Fig 2. The experimental setup includes a three-phase 5-kW PWM-VSC, which is supplied from a constant DC voltage and connects to a grid simulator at the AC side. Moreover, the proposed control method is realized in a DS1007 dSPACE system. The parameters of the simulated and experimental systems are the same and given in Table. I.

Table I: System parameters

Nominal power	5 [kVA]
Nominal phase voltage	230 [V]
Grid frequency	50 [Hz]
Inverter-side inductor (L_f)	3 [mH]
Grid-side inductor (L_g)	3 [mH]
Filter capacitor (C_f)	20 [µF]
DC-link voltage (V_{dc})	720 [V]
Sampling period (T_S)	25 [µsec]
Control parameters	
k_d	0.1
λ_{sw}	1000
Observer eigenvalues	[0.01,0.01,0.99,0.05]

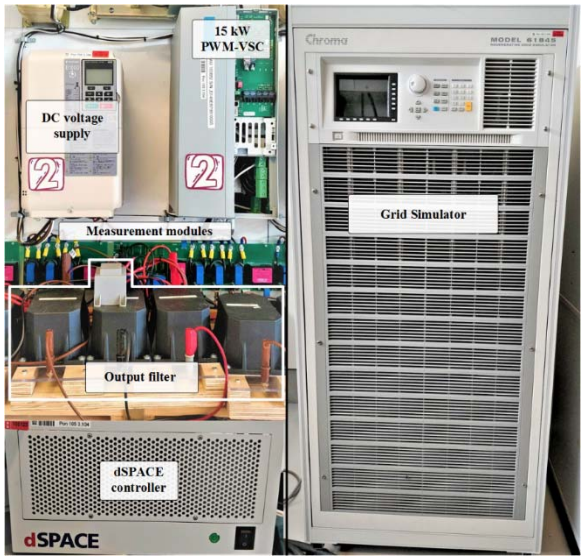

Fig. 2: Laboratory setup used to verify the effectiveness of proposed P-DPC

In the first study, the steady-state performance of the proposed method is presented in Fig. 3. Highly sinusoidal grid currents and regulated injected active and reactive powers with minimum distortions are seem. It is worth note that the average switching frequency of the proposed control method is 3.4 kHz, which is acceptable in point of the switching losses. Although the switching frequency is approximately low, however the total harmonic distortion (THD) of the grid current is 3.8%, which well satisfies the international standard, such as IEEE 519.

To compare performance of the proposed sensorless P-DPC with the conventional P-DPC, the performance of the conventional one is also shown in Fig. 4. It is worth to remark that the conventional P-DPC uses additional sensors for grid-side currents. It can be concluded from Figs. 3 and 4 that both control methods have the same performance.

The transient performance of the proposed adaptive P-DPC and conventional one under consecutive reference power changes is presented in Fig. 5, which shows the performance of both control methods to track the reference powers rapidly. It is worth to point out that this excellent operation is achieved without using any grid current and voltage sensors, and all previous results are obtained using the LO algorithm in the control structure. In Fig. 6, the excellent performance of the LO to estimate the system states and disturbance inputs is shown.

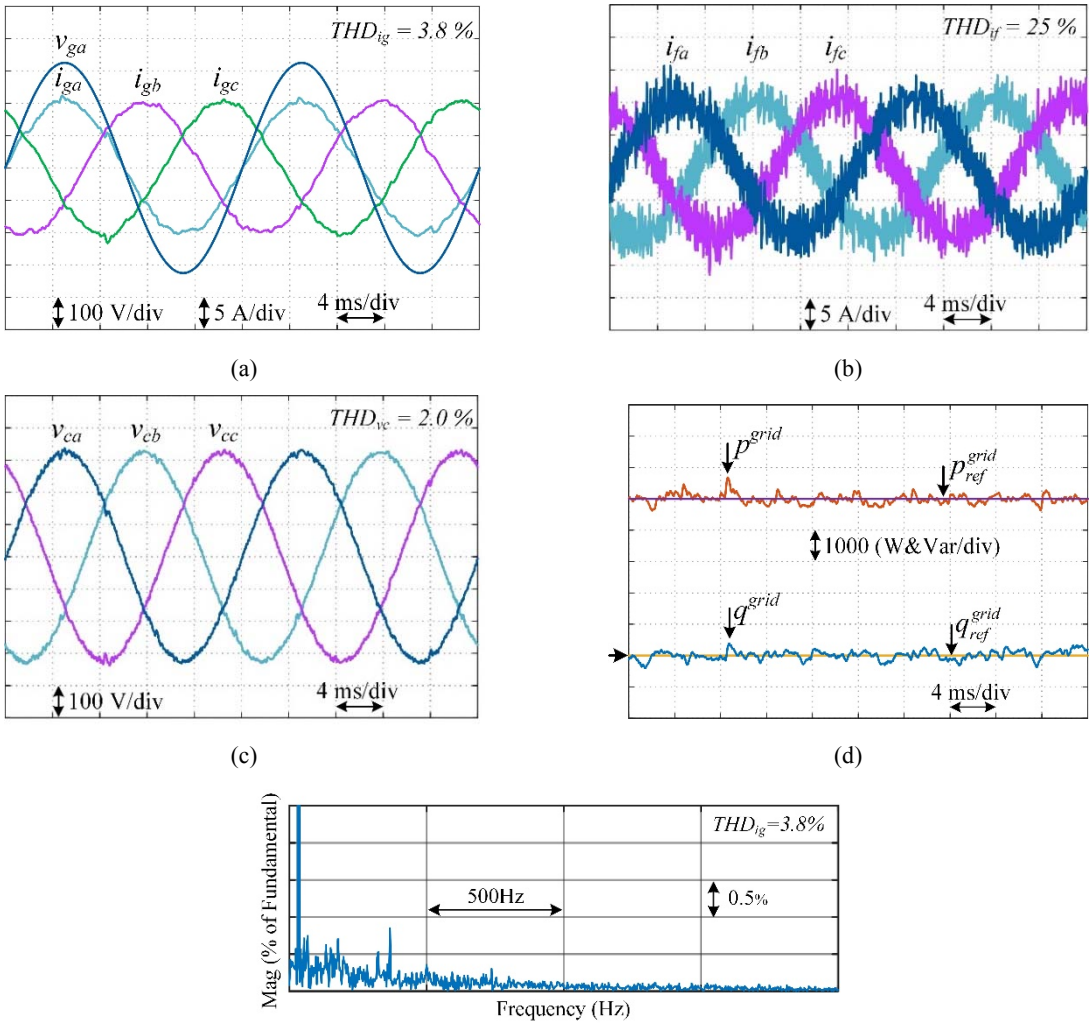

Fig. 3: Simulation results showing steady-state performance of the proposed adaptive P-DPC (P = 5 kW, Q = 0 Var), (a) grid voltage and currents, (b) inverter currents, (c) capacitor voltages, (d) grid active and reactive powers, (e) (d) harmonic spectrum of the grid current.

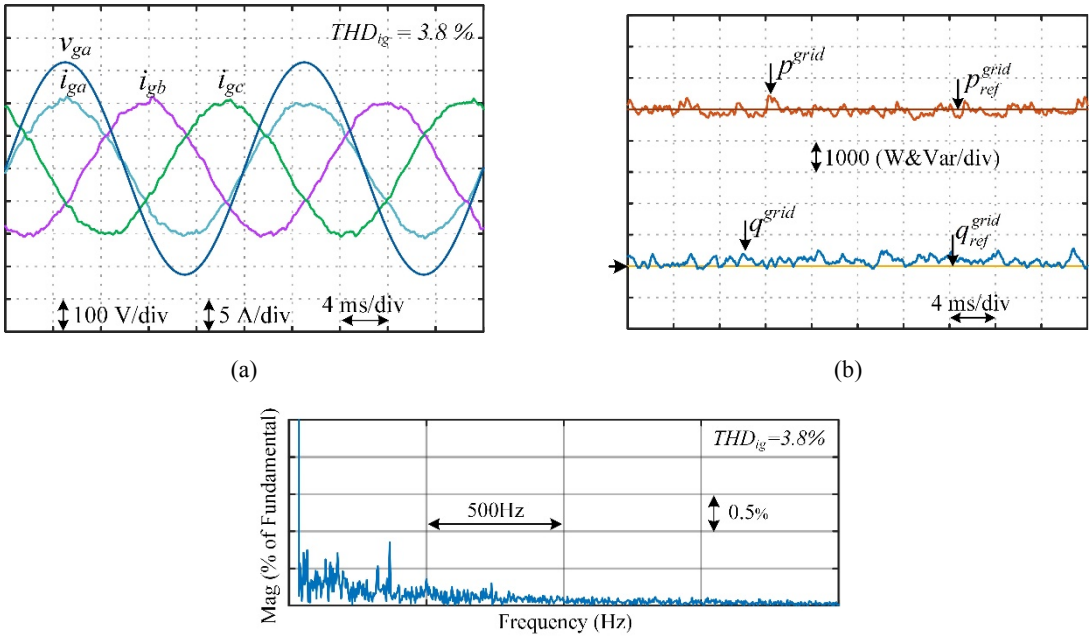

Fig. 4: Simulation results showing steady-state performance of the conventional P-DPC (P = 5 kW, Q = 0 Var), (a) grid voltage and currents, (b) grid active and reactive powers, (c) capacitor voltages, (d) harmonic spectrum of the grid current.

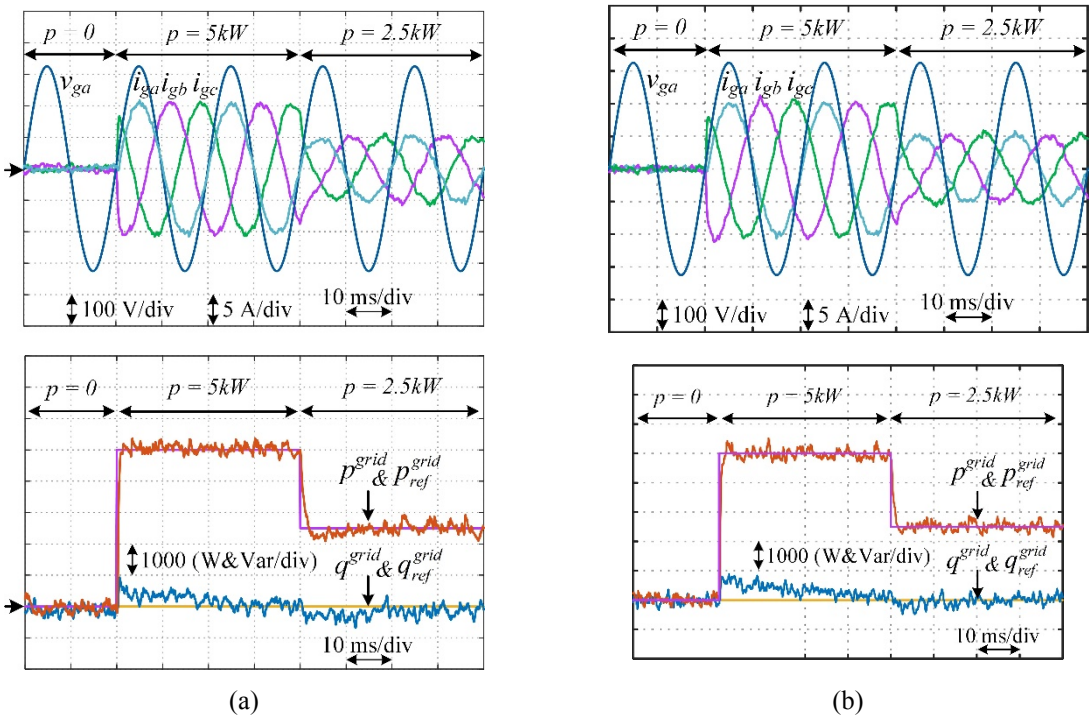

Fig. 5: Simulation results showing dynamic performance in response to reference power step changes (Q = 0 Var), (a) proposed adaptive P-DPC, (b) conventional P-DPC.

To validate the feasibility of the proposed adaptive P-DPC, experiments are carried out on a laboratory setup. Fig. 7 depicts the steady-state waveforms of the grid currents under pure sinusoidal grid voltages. This figure confirms the high capability of the proposed control method to achieve the sinusoidal current generation and perfect active and reactive power regulation. Fig. 8 shows the dynamic response of the proposed control methods under the step changes in the reference active power as in the simulations.

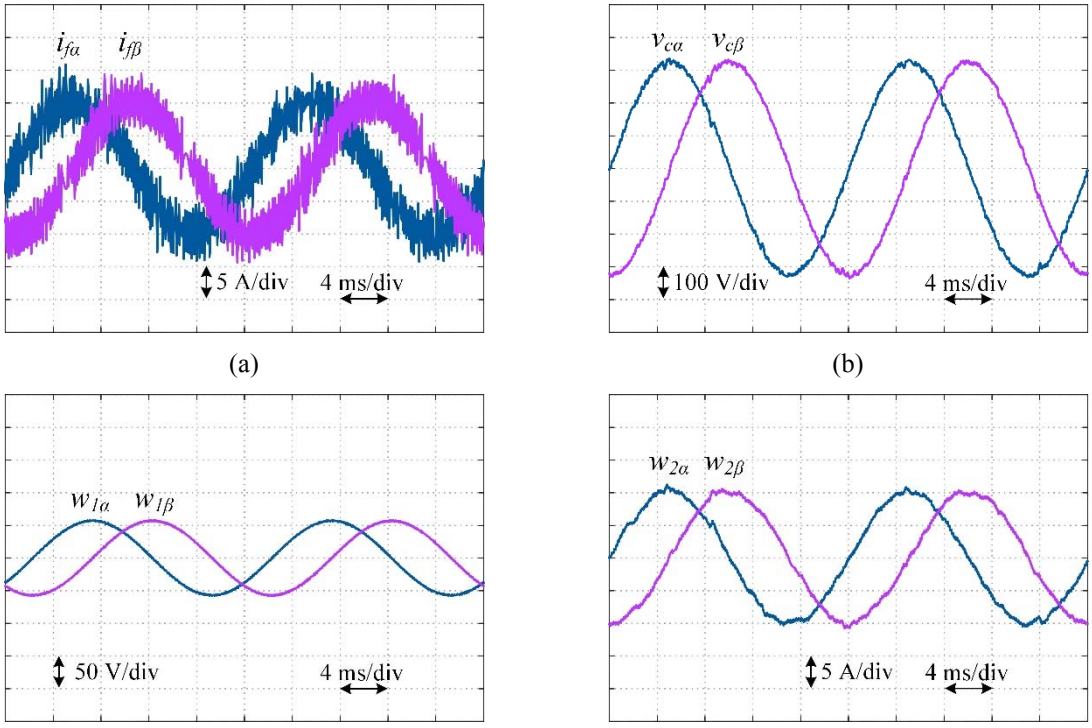

Fig. 6: Simulation results showing outputs of the proposed Luenberger observer (a) estimated inverter currents, (b) estimated capacitor voltages, (c) and (d) estimated disturbance inputs.

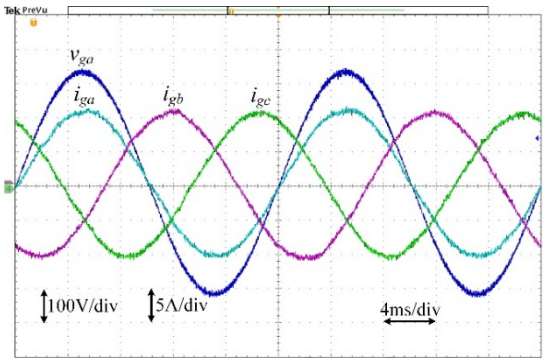

Fig. 7: Experimental results showing steady-state performance of the proposed adaptive P-DPC (P = 5 kW, Q = 0 Var).

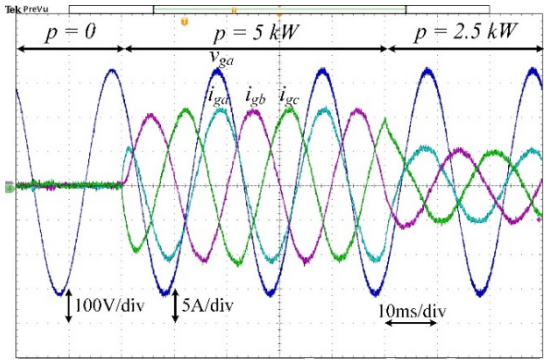

Fig. 8: Experimental results showing dynamic performance of the proposed adaptive P-DPC in response to reference power step changes (Q = 0 Var)

Conclusion

In recent years, due to the availability of powerful digital signal controllers (DSCs), more attentions are paid to predictive based control methods. A special application for the predictive methods is the renewable energy-based distributed power generation systems, where bidirectional power flow control is required. However, these methods are susceptible to system control delays and parameter variations and need too many current and voltage sensors. In this study, an improved P-DPC is proposed, which utilizes a LO to improve the system performance by compensating for delays and parameter drifts and uncertainties. Also, the number of sensors is successfully reduced by replacing some of them with estimation already provided by the LO. The performance of the proposed adaptive P-DPC is evaluated under different operation conditions. Simulation and experimental results confirm the superior performance of the proposed method under various conditions.

References

[1] T. Dragicevic, C. Zheng, J. Rodriguez and F. Blaabjerg, "Robust quasi-predictive control of LCL-Filtered Grid Converters," *IEEE Trans. Power Electron.*, vol. 35, no. 2, pp. 1934-1946, Feb. 2020.

[2] P. Falkowski and A. Sikorski, "Finite control set model predictive control for grid-connected AC-DC converters with LCL filter," *IEEE Trans. Ind. Electron.*, vol. 65, no. 4, pp. 2844–2852, 2018.

[3] X. Zhang, L. Tan, J. Xian, H. Zhang, Z. Ma and J. Kang, "Direct grid-side current model predictive control for grid-connected inverter with LCL filter," *IET Power Electron.*, vol. 11, no. 15, pp. 2450-2460, 18 12 2018.

[4] S. Zhou et al., "An improved design of current controller for LCL-type grid-connected converter to reduce negative effect of PLL in weak grid," *IEEE J. Emerg. Sel. Top. Power Electron.*, vol. 6, no. 2, pp. 648-663, June 2018.

[5] C. A. Busada, S. G. Jorge and J. A. Solsona, "A synchronous reference frame PI current controller with deadbeat response," *IEEE Trans. Power Electron.*, vol. 35, no. 3, pp. 3097-3105, March 2020.

[6] H. Wu and X. Wang, "Virtual-flux-based passivation of current control for grid-connected VSCs," *IEEE Trans. Power Electron.*, doi: 10.1109/TPEL.2020.2997876.

[7] H. Gholami-Khesht, M. Monfared, and S. Golestan, "Low computational burden grid voltage estimation for grid connected voltage source converter-based power applications," *IET Power Electron.*, vol. 8, no. 5, pp. 656-664, May. 2015.

[8] Y. Zhang, W. Xie, Z. Piao and C. Hu, "Performance improvement of direct power control of PWM rectifier with simple calculation," *IEEE Trans. Power Electron.*, vol. 28, no. 7, pp. 3428-3437, Jul. 2013.

[9] L. A. Serpa, S. Ponnaluri, P. M. Barbosa and J. W. Kolar, "A modified direct power control strategy allowing the connection of three-phase inverters to the grid through LCL filters," *IEEE Trans. Ind. Appl.*, vol. 43, no. 5, pp. 1388-1400, Sept. 2007.

[10] L. A. Serpa, J. W. Kolar, S. Ponnaluri and P. M. Barbosa, "A modified direct power control strategy allowing the connection of three-phase inverter to the grid through LCL filters," *Industry Applications Conference*, vol. 1, pp. 565-571, 2005.

[11] H. Li, M. Lin, M. Yin, J. Ai and W. Le, "Three-vector-based low-complexity model predictive direct power control strategy for PWM rectifier without voltage sensors," *IEEE J. Emerg. Sel. Top. Power Electron.*, vol. 7, no. 1, pp. 240-251, March 2019.

[12] X. Shi, J. Zhu, L. Li and D. Dah-Chuan LU, "Low-complexity dual-vector-based predictive control of three-phase PWM rectifiers without duty-cycle optimization," *IEEE Access*, vol. 8, pp. 77049-77059, 2020.

[13] A. M. Bozorgi, H. Gholami-Khesht, M. Farasat, S. Mehraeen and M. Monfared, "Model predictive direct power control of three-phase grid-connected converters with fuzzy-based duty cycle modulation," *IEEE Trans. Ind. Appl.*, vol. 54, no. 5, pp. 4875-4885, Sept.-Oct. 2018.

[14] S. Yan, J. Chen, T. Yang and S. Y. Hui, "Improving the performance of direct power control using duty cycle optimization," *IEEE Trans. Power Electron.*, vol. 34, no. 9, pp. 9213-9223, Sept. 2019.

[15] P. Karamanakos and T. Geyer, "Guidelines for the design of finite control set model predictive controllers," *IEEE Trans. Power Electron.*, vol. 35, no. 7, pp. 7434–7450, Jul. 2020.

[16] V. Miskovic, V. Blasko, T. M. Jahns, A. H. C. C. Smith, and C. Romenesko, "Observer-based active damping of LCL resonance in grid-connected voltage source converters," *IEEE Trans. Ind. Appl.*, vol. 50, no. 6, pp. 3977–3985, Nov. 2014.

[17] H. Gholami-Khesht and M. Monfared, "Deadbeat direct power control for grid-connected inverters using a

full-order observer," *Electric Power and Energy Conversion Systems* (EPECS), pp. 1-5, Sharjah, 2015.

[18] Y. A. R. I. Mohamed and E. F. El-Saadany, "Robust high bandwidth discrete-time predictive current control with predictive internal model - A unified approach for voltage-source PWM converters," *IEEE Trans. Power Electron*., vol. 23, no. 1, pp. 126–136, Jan. 2008.

[19] N. Hoffmann and F. W. Fuchs, "Minimal invasive equivalent grid impedance estimation in inductive–resistive power networks using extended Kalman filter," *IEEE Trans. Power Electron*., vol. 29, no. 2, pp. 631–641, Feb. 2014.

[20] Y. A.-R. I. R. I. Mohamed and E. F. El-Saadany, "Adaptive discrete-time grid-voltage sensorless interfacing scheme for grid-connected DG-inverters based on neural-network identification and deadbeat current regulation," *IEEE Trans. Power Electron*., vol. 23, no. 1, pp. 308–321, Jan. 2008.

[21] Y. A. R. Ibrahim Mohamed et al., "An improved deadbeat current control scheme with a novel adaptive self-tuning load model for a three-phase PWM voltage-source inverter," *IEEE Trans. Ind. Electron*., vol. 54, no. 2, pp. 747–759, Apr. 2007.

[22] Q. Liu and K. Hameyer, "High-performance adaptive torque control for an IPMSM with real-time MTPA operation," *IEEE Trans. Energy Convers*., vol. 32, no. 2, pp. 571–581, Jun. 2017.